CHALMERS
UNIVERSITY OF TECHNOLOGY

Improved material performance in floorball sticks

Implementation of the Finite Element Method for helically fiber-oriented laminae in cylindrical hollow composites

Master thesis in Applied Physics

MATS LINDSTRÖM

Improved material performance in floorball sticks

Implementation of the Finite Element Method for helically fiber-oriented laminae in cylindrical hollow composites

MATS LINDSTRÖM

Improved material performance in floorball sticks
Implementation of the Finite Element Method for helically fiber-oriented laminae in cylindrical hollow composites
MATS LINDSTRÖM

Improved material performance in floorball sticks
Implementation of the Finite Element Method for helically fiber-oriented laminae in cylindrical hollow composites

MATS LINDSTRÖM
Department of Applied Physics
Division of Condensed Matter Physics
Chalmers University of Technology

Sammanfattning

Då innebandy är en relativt ny sport är mängden forskning specifikt ämnat åt att utveckla denna begränsad. Trots att omfattande forskning genomförs gällande kompositmaterial har endast ett fåtal projekt inriktat sig på de högst specifika geometrier och belastningar som gör sig gällande på innebandyklubbornas skaft vid spel. Anpassning av denna forskning kan i förlängningen leda till förbättrade materialegenskaper och därmed reducera skaderisken för utövarna av sporten. Målet med detta projekt var att utveckla kod som kan användas för att undersöka om förändrad sammansättning och struktur av kompositmaterialen i innebandyklubbor kan öka dess slagtålighet och därmed minska skaderisken. Baserat på grundläggande koncept inom läran om kompositer såsom homogenisering, linjär elasticitet och transformation av koordinatsystem har en implementation av Finita Elementmetoden (FEM) skapats och använts för att illustrera hur varierande av fiberskiktvinklar i skruvlinjeformade lameller påverkar materialegenskaperna i cylindriska kompositer. Existerande data från rörelseanalysmätningar och experimentella värden för elasticitetsmodulen i innebandyklubbor användes som referens för att styrka resultaten från simuleringarna. Simuleringarna visade slutligen hur skiktvinklarna påverkar böjen på klubbskaftet. Än viktigare är dock möjligheten att återanvända koden för andra undersökningar av materialstrukturen såsom varierande av andelen fiber och gjutmaterial, ordningsföljden i staplingen av lamellerna samt olika lastfall.

Abstract

As a relatively novel sport, the amount of research specifically aimed at developing the game of floorball is limited. Despite the extensive research efforts being carried out related to composite materials few of the developed methods have yet to be adapted to the highly specific geometries and load-cases which apply to floorball stick shafts in play. Adaptation of these methods could ultimately lead to improved material performance and thus reduce the risk of injury for the athletes. The aim of this project was to develop a code base which can be implemented to investigate if improvements in the composition of the composite materials used in floorball stick shafts can be made to increase the impact resistance and thereby reduce risk of injury. Based on fundamental composite concepts such as homogenization, linear elasticity an coordinate system transformations an implementation of the Finite Element Method (FEM) was created and used for illustrating how varying the ply angles in helically oriented laminae affect the material properties in composite cylinders. Existing data from movement analysis measurements and experimental values of the elastic modulus for floorball sticks were used as a reference to validate the simulations. The simulations ultimately resulted in showing how deflections resulting from loads applied to cylindrical composites depend on the ply angles of the laminae. Even more important, however, is the reusability of the FEM implementation for other variations of the material structure such as volume fractions of fiber and matrix, lamina stacking sequence and ply angles, as well as different load-cases.

Preface

The project described in this report was conducted as a Master thesis at Chalmers University of Technology during 2015, within the Department of Applied Physics. It resulted in an implementation of the Finite Element Method for cylindrical, circular hollow tubes, the source code of which can be found and retrieved from `https://github.com/MatsLindstrom/FEM_CFRP_hollowCylinders`.

The completion of this project would not have been possible without the support and inspiration given by Associate Professor Magnus Karlsteen from the Department of Applied Physics at Chalmers University of Technology. As supervisor of this project, much gratitude is owed to Magnus for introducing me to the field of Technology in Sport and the opportunities that lie within.

The support given by friends and family has been overwhelming, and has encouraged me to push my own personal development further than I imagined possible.

Appreciation is also owed to researchers and staff at Chalmers, not least those involved in the Sports Technology venture, who are always willing to share their knowledge and technical expertise.

Gothenburg, October 2015

Mats Lindström

List of terms and acronyms

Matrix Binding material

Precursor Initial material before preparation

Resin Polymer precursor

Fiber Reinforcing material

Filament Single thread of fiber

Roving/tow A bundle of filaments

Ply/lamina Layer of laminated material

Laminate A stack of plies/laminae

Angle-ply Set of plies oriented at opposing angles $\pm\theta$, *i.e.* mirrored relative to principal direction of the laminate

Cross-ply Set of plies oriented at $0°$ and $90°$ only, relative to principal laminate direction

Balanced laminate Laminate consisting of pairs of plies with equal thickness but mirrored orientation along the laminate principal direction

Symmetric laminate Ply thicknesses and orientation mirrored with respect to the midplane

Weave Layer of interwoven fibers

Anisotropy Directional dependency

Monoclinic One plane of material symmetry

Orthotropic Two planes of material symmetry

FEM/FEA Finite Element Method/Analysis

IFF International Floorball Federation

CLT Classical Lamination Theory

Contents

1

Introduction

In the following introduction, the topic, aim and objective of this thesis is defined and clarified. Finally, the structure of this document is described.

1.1 Background

For many years the rapid technological development in sports has attracted the attention of industry and academia. As of 2015, Chalmers University of Technology together with University of Gothenburg is classified as a national sports university, which shows the increased efforts put into research in the field [1]. Among the main sports researched in this venture is floorball [2].

Floorball is a rapidly expanding sport in Europe and the world today, and since the founding of the International Floorball Federation (IFF) in Sweden in 1986 the organization has grown to include 58 member associations from all over the world [3].

As the sport develops, so must also the technology and materials used in the sporting utilities. The IFF has set a number of restrictions on this development in order to maintain the quality of game play [4], but potential for material improvement is far from gone. The evolution of technology used in sport can, among other things, reduce risk of injuries as well as increase public health as an indirect effect from raising the public interest in exercising by improving the overall quality of the game.

The strain applied to floorball sticks during game play requires flexible, strong and light weight materials. An optimal combination of these properties would increase the speed and quality of the game, while reducing the risk of harmful stick breakage. Today, most of the materials used in sports are relatively complex, and a large part of these materials consist of fiber composites and reinforced plastics. Not only are fiber composites suitable due to their excellent strength to weight ratio, they can also be designed to absorb impacts in a way so that cracking does not lead to complete material failure. [5]

Numerous attempts to optimize the properties of reinforced plastics for specific applications have been conducted and are continuously refined [5, 6, 7, 8, 9]. Although the theory of composite materials is well developed, there has in the past been little to no previous scientific research within the university community regarding floorball, mostly due to its relatively novel introduction to the world of sports, but also due to a general mismatch be-

tween the scientific community and the sporting industry. There exists, however, a strong desire to develop scientific methods for improving the sport.

Furthermore, empirical testing of composites is by far the simplest method for investigating properties such as stiffness and strength, but it is tedious and the results are only valid for the specific testing conditions and the fiber being tested. Thus, more generalized methods for testing and analyzing materials are desirable. A large number of software suites have been developed to make the research efforts more effective, but most of these act as a form of black box, giving the user little insight in the mechanisms behind the solver implementation.

1.1.1 Floorball

As described in [10], floorball is officially played between two teams of six players each, preferably indoors on a hard and even surface inside a rink of dimensions $40\,\mathrm{m} \times 20\,\mathrm{m}$. During the duration of the game, normally consisting of 3 periods á $20\,\mathrm{minutes}$, the aim is to score more goals than the opposing team. This is achieved by passing a hollow plastic ball within the team using floorball sticks (*c.f.* figure 1.1) and attempting to shoot the ball into the opposing teams goal.

Figure 1.1: Typical floorball stick, certified by IFF

Existing regulations

In order to control the development of the game, SP Technical Research Institute of Sweden has developed a set of certification rules for materials used on behalf of IFF. In the present moment, the latest version of certification rules can be found in [4].

Some material regulations relevant for this project are listed in table 1.1 for convenience.

Table 1.1: List of relevant material properties for the stick shaft according to [4]

Property	Regulated value
Total stick weight	Maximum $380\,\mathrm{g}$
Stick length	Maximum $1140\,\mathrm{mm}$
Stick shaft curve radius	Minimum $6\,\mathrm{mm}$
Stick shaft diameter	Maximum $35\,\mathrm{mm}$
Stick shaft straightness	Within $50\,\mathrm{mm}$

Furthermore, the requirements of shaft flexibility depends upon the length of the stick, according to the following.

$\geq 850 \, \text{mm}$: minimum deflection of $23 \, \text{mm}$ under load of $300 \, \text{N}$ as a mean value of three deflections. At least $60 \, \text{mm}$ deflection in the most flexible direction without cracking or fracturing.

$< 850 \, \text{mm}$: minimum deflection of $10 \, \text{mm}$ under load of $300 \, \text{N}$ as a mean value of three deflections. At least $30 \, \text{mm}$ deflection in the most flexible direction without cracking or fracturing.

1.1.2 Composites used in sporting goods

There are a growing number of floorball equipment manufacturers on the market today, and besides varying the geometry of the shaft to enhance performance a number of different material combinations are employed to increase strength and reduce weight of the stick. In general, the highest performance-rated sticks offered on the market normally consist of a mixture of carbon and glass fiber composites. [11, 12, 13, 14, 15]

As an example, the floorball equipment manufacturer in [15] produces a variety of carbon fiber reinforced floorball sticks, using composites with varying strengths, from fiber tensile strengths of approximately $2200 \, \text{ksi} \approx 15.2 \, \text{GPa}$ and downward.

The structure of the fiber weave also varies, from plain weave to multidirectional fiber weaves, examples of which can be seen in figure 1.2. A closer look at these samples reveal that they consist of approximately cross-ply weaves degrees for two of the samples and angle-ply weaves ($[\pm 45]$) for the third.

Figure 1.2: Samples of broken floorball sticks

Composite materials are also widely used in other sports, out of which pole vaulting is a good example to compare with, since the geometry of a pole resembles that of a floorball stick shaft. From [5], a pole vault usually consists of three layers of fibers: an outer layer of carbon fibers, an intermediate layer of glass fiber web and an inner layer of glass fiber

rings. The combination of these layers give the pole excellent resilience to tensile and torsional forces, while keeping the weight of the pole to a minimum. Other equipment where the use of reinforced plastic composite materials has been successful range from rackets for badminton and tennis to boat hulls and masts for high-performance sailing.

The most important fiber types used in sporting goods today consist of carbon, but also glass, aramid, polyurethane and boron are common and the market is constantly searching for alternative materials.

For all of the aforementioned sports the industry has combined different composites in numerous mixtures and fiber orientations to achieve the optimal design most suitable for its intended use. [5]

1.1.3 Existing data and past research

The sports technology venture at Chalmers University of Technology has produced a number of research projects (*e.g.* [8],[16]) which can be used as a basis for the present work. For example, it has been shown in [16] that a typical slapshot in floorball is equivalent to exerting a force of more than $700\,\mathrm{N}$ to the end of the stick. The venture has also inspired collaboration between academia and industry, such as the one between Chalmers and Qualisys, among other opportunities leading to access to movement analysis data from slapshots performed by professional floorball players.

In order to maintain a strong connection to real life situations, approximate values used in this report are based on those of a reference floorball stick and can be seen in table 1.2. The reference stick from which these values were obtained was also used for the experimental measurements.

Table 1.2: Approximate reference stick dimensions

Property	Value
Stick shaft length from top to blade	$0.975\,\mathrm{m}$
Stick shaft length for 3 point bending	$0.95\,\mathrm{m}$
Stick shaft length from lower grip to blade	$0.46\,\mathrm{m}$
Stick shaft outer radius	$10\,\mathrm{mm}$
Stick shaft composite thickness	$1.5\,\mathrm{mm}$
Stick shaft straightness	Within $1\,\mathrm{mm}$

1.2 Purpose

The purpose of this thesis is to investigate methods for improving the overall material performance in floorball sticks, thereby making the sport more attractive and safe. It shall also provide a sufficient framework for future development and research.

In the final stage of the project the following questions shall be answered:

Can the performance of floorball sticks be accurately modeled using the Finite Element Method? If so, how does the fiber alignment of the plies affect the stick at pure bending?

1.3 Scope

This project entails a literature review and research (including laboratory testing and computer simulations) focused on composite materials currently in use or suitable for future use in floorball sticks, but does not include any physical production of materials nor the manufacturing of new prototypes. Economical aspects and manufacturing details are thus not taken into account in the procedure.

The purpose of this thesis can be achieved in many ways, *e.g.* by investigating composite microstructure, geometric shapes or fatigue life. The chosen methods are presented in detail in chapter 3 along with the reasoning behind the choices. In short, the simulations presented herein focused on cylindrical, hollow tubes of laminates with angle-ply stacking, and the desired result was to investigate the effects of varying the angles of the plies on the stick shaft properties.

Although many different software suites designed for modeling materials are available on the market, this thesis investigates material properties mainly by implementation of Finite Element Analysis (FEA). This was done due to the author's will to learn more about common algorithms used during FEA implementation, and the desire to gain deeper insight into the application of FEA as a whole.

The scope of the project is further narrowed down by a number of assumptions, presented in detail in section 3.2.1, thereby making the modeling more general and adaptable as well as simpler and more computationally efficient.

In recent development curved sticks have become increasingly popular. However, this report focused on the modeling of straight sticks only. Furthermore, material uncertainties arising from imperfections such as fiber misalignment or weak bonding between matrix and fiber can strongly affect the results of the material performance in practical use. These eventualities are not taken into account in the current computational model, resulting in a uncertainty in the result. [7]

1.4 Thesis outline

This report begins with a theoretical outline in chapter 2, covering fundamental theory related to reinforced plastics. A closer look into rudimentary composite mechanics needed for the computational procedure is given in section 2.3, supported by the more detailed expressions given in appendices A and B.

The overall project procedure is given in chapter 3, where section 3.1 describes the experimental procedure and section 3.2 details the computational methods used for the simulations, also supported by the appendices.

Chapter 4 shows the results of both the experimental measurements and the numerical

simulations using FEA, as well as the deflections obtained from movement analysis data. The latter result is supported by figures given in appendix C.

A comparison of the obtained results is given in chapter 5, and error estimates are approximated and analyzed. Furthermore, suggestions and recommendations for further research is given in section 5.3.

Finally, conclusions from the obtained results and discussions are drawn in chapter 6.

2

Theory

The following chapter outlines the basics of reinforced plastics, as well as the existing market. Furthermore, definitions of terms related to the field as well as relevant mechanical theory is introduced. Finally, commonly used computational methods for optimizing performance of fiber reinforced materials are briefly presented, together with necessary theory governing FEA.

2.1 Reinforced plastics

In modern applications, reducing the weight to strength ratio of the materials used while maintaining a low production cost is an increasingly important aspect in design considerations. Composite materials such as reinforced plastics are, because of their excellent weight to strength ratio, constantly growing more important in fields such as aviation, automotive and sports, where strong, light-weight materials are a crucial part of improving performance. [5]

Reinforced plastics normally consist of two constituents, the polymer matrix, used to bind the material together, and the fiber reinforcement, used for strengthening the material, much like armaments are used to reinforce concrete structures. [17]

In general, the properties of composite materials depend on the properties of their constituents, e.g. concentrations, distributions and orientation, but also the physical and chemical interactions between constituents. The most relevant aspects to take into consideration for numerical optimization are normally considered to be the fiber orientation, stacking sequence and layer thickness of the composite layers (laminae).

Although increased layer thickness naturally can make a material more durable, the constraints on weight and dimensions in floorball sticks deems this method of optimization less relevant. It should also be mentioned that while symmetric structures lead to simplified analysis and reduces unwanted coupling effects, they also lead to increased weight of the structure, something that has to be considered in the simulation procedure. [7]

In general, the material properties of interest in sporting goods can be summarized as follows [5]:

- strength (tensile, torsional, compressive, shear)

- lightness
- stiffness (low deflection)
- fatigue resistance (reduce risk of failure under cyclic loading)
- dampening under impact
- fracture toughness (reduce risk of sudden failure)

2.1.1 Basic definitions

A laminate typically consists of several lamina, or plies, stacked or woven in a certain pattern. The orientation of the fibers in a laminate can be described by a set of angles, normally with the reference direction $\theta = 0$ being the direction of the main applied load. As a simple example, $[+45/0/-45]$ represents three plies stacked on top of each other, where the bottom ply is at a positive $45°$ angle relative to the reference direction. [17] In the case of a symmetric ply, such as $[+45, 0, +45]$, the subscript s is used to simplify the notation as $[+45, 0]_s$, and in the anti-symmetric case the subscript a is used, *e.g.* $[+45, 0]_a = [+45, 0, -45]$. To shorten the notation further, an integer subscript is here used to represent the repetition of the same ply angle, *e.g.* $[+45]_3 = [+45, +45, +45] = [+45_3]$, and $\pm$ indicates alternating positively and negatively oriented plies.

A sketch of a simple $[+45, 0]_a$ composite can be seen in figure 2.1, along with the definition of longitudinal and transverse directions to the fibers. Further examples of common fiber patterns can be found in [5], including examples of woven, knitted and braided composites.
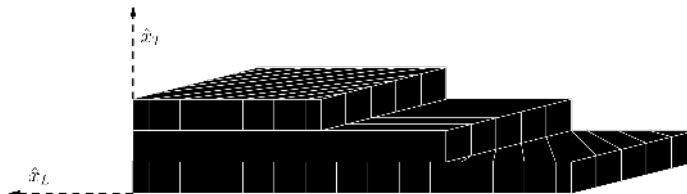

Figure 2.1: Sketch of stacked laminae, along with definition of longitudinal and transverse directions

2.1.2 Polymer matrix

When choosing the type of polymer matrix to be used, one of the most crucial aspects to consider is what methods of production are available and the quality of the product these methods can maintain. For items of substantial volume, thermosets such as thermoset polyesters have long been the preferred matrix due to their relatively low cost. When need to increase the mechanical performance of the material increases, a common choice

is instead epoxies. For smaller items, where precision is required, thermoplastic matrices hold a large part of the market due to the possibility to form the objects via the relatively cheap injection-molding or extrusion processes. [17]

Since the properties of the matrix generally determines the strength in the fiber composites' transverse direction, the material strength in these directions are inherently small. Thus, the importance of orienting the fibers correctly increases.

2.1.3 Fiber reinforcements

A large number of reinforcing fibers of different materials and form exist on the market today, and the choice of fiber is closely related to the intended application and the requirements on, to mention just a few of the parameters, cost, strength and weight.

Each filament of the fiber typically has a cross-section with a diameter of around $5\,\mu m$ to $15\,\mu m$, and the fibers are normally bundled together into so called rovings or tows [17]. The length of the fibers can vary, from the use of carbon nanotubes to high modulus fibers several thousands of Ångström in length [18, 19, 20].

The most common types of reinforcements today are glass fibers, carbon fibers and oriented polymeric fibers, each with their own advantages for different applications. While glass fibers, made out of inorganic glasses based on silica, show resistance to high temperatures, are transparent to visible light and intrinsically isotropic, they are prone to fatigue, vulnerable to surface damage caused by *e.g.* moisture and crystallinity in the material greatly reduces its strength.

A well known fact in the scientific community is that graphite lattice planes persist over very large distances despite curvature, leading to extraordinary tensile strength and high modulus thus explaining the interest in carbon fiber materials [21]. Orienting the fibers along the direction of the applied strain and thus making the material stronger in certain directions has become an increasingly popular, albeit expensive method, and it is today widely employed using for example polyacrylonitrile (PAN) and aramid precursors. In general, higher degree of orientation of the fibers leads to higher modulus of the material [22, 23]. The concentration of the fibers as well as the degree and direction of orientation can, using these polymers, be customized to the application, a major advantage when quality needs to be ensured. Carbon fibers show an especially impressive resistance to fatigue, stability and chemical inertness, making it an excellent choice for long-term use in many demanding applications.

Due to the chemical structure of most polymers, it is difficult to achieve a high degree of orientation, making carbon fibers difficult and expensive to produce. Using aramid polymers, however, a relatively high degree of orientation can be obtained. Because of this, aramid polymers are becoming an increasingly popular choice, of which the most well-known ought to be the Kevlar fiber. Although strong and relatively durable, these materials show a weakness in axial shear. [17]

Properties of some common fibers can be seen in table 2.1. It should be noted, however, that these values are only representative for a few very specific materials, the value of a general fiber material is greatly affected by parameters mentioned above such as the

degree and direction of orientation and the precursor used to produce the fibers. [22]

Table 2.1: Properties of common fiber materials, from [5]

Property	Kevlar	E-glass	Carbon	SiC	Polyethylene
Mean fiber diameter [μm]	0.2	0.2	0.1	0.14	5×10^{-2}
Density [Mgm^{-3}]	1.44	2.54	1.8	3.0	0.97
Tensile (Young's) modulus [GPa]	124	72	220	40	120
Tensile strength [GPa]	2.76	3.45	2.07	4.83	2.59
Elongation to fracture [%]	2.4	4.8	1.2		3.8

For a typical carbon/epoxy reinforced plastic of type T300/LY5052 the 9 independent material properties required for the material stiffness matrix of an orthotropic material can be seen in table 2.2. [9]

Table 2.2: Typical values of material properties for carbon/epoxy (T300/LY5052) composite, from [9]

Property	Value	Unit
E_1	135.0	GPa
$E_2 = E_3$	8.0	GPa
$G_{12} = G_{13}$	3.8	GPa
G_{23}	2.7	GPa
$\nu_{12} = \nu_{13}$	0.27	-
ν_{23}	0.49	-

2.2   Simple bending of beams

Fundamental mechanics can provide relatively simple approximations of the deflections experienced during the bending of beams. Under three point bending, *i.e.* a load applied to the middle of the beam while resting freely on two supports, deflection at the center of the beam is given by $w(L/2) = PL^3/48EI$, where P is the applied force and L, E and I is the length, flexural modulus and area moment of inertia of the beam, respectively. Similarly, for a fixed beam with one free, loaded end, the deflection is given by $w(L) = PL^3/3EI$. Combining these two equations, eliminating E and I, leads to

$$\frac{P_{3p}L_{3p}^3}{48w_{3p}\left(L_{3p}/2\right)} = \frac{P_{fix}L_{fix}^3}{3w_{fix}\left(L_{fix}\right)} \quad \Rightarrow \quad w_{fix}\left(L_{fix}\right) = 16\frac{P_{fix}}{P_{3p}}\frac{L_{fix}^3}{L_{3p}^3}w_{3p}\left(L_{3p}/2\right) \quad (2.1)$$

where the subscript fix represents a beam with one fixed end while $3p$ stands for the three point bending case.[24]

2.3 Composite mechanics

A wide range of parameters affect the mechanical properties of composites, such as stacking orientation and sequence, overall fiber volume fraction, weave architecture and yarn spacing. The problem of optimizing the properties of a composite thus has to be simplified. In the following a basic case of cylindrical, stacked, monoclinically symmetric plies is considered as a foundation for the simulations. A sketch of the considered geometry can be seen in figure 2.2.
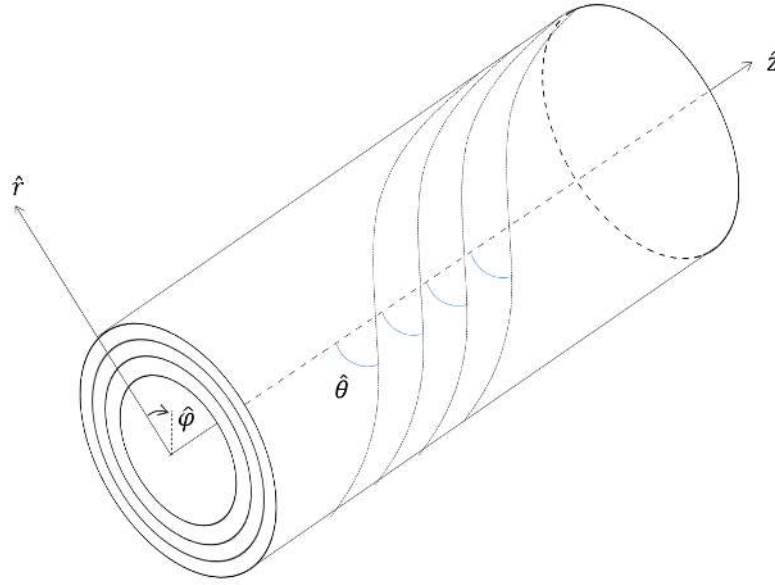

Figure 2.2: Geometry of cylindrical composite shell with helically oriented fibers with angle θ relative to cylinder $\hat{z}$-axis

2.3.1 Governing equations

The deformation of a linear elastic material under externally applied loads can be described by combining three governing equations.

The first equation to consider is termed the strain-displacement ($\boldsymbol{\varepsilon} - \boldsymbol{u}$) relation and can, in a cartesian coordinate system and tensor notation, be expressed as

$$\varepsilon_{ij} = \frac{1}{2}\left(\frac{\partial u_i}{\partial x_j} + \frac{\partial u_j}{\partial x_i}\right), \quad i,j \in \{1,2,3\}. \tag{2.2}$$

Secondly, the stress-strain ($\boldsymbol{\sigma} - \boldsymbol{\varepsilon}$) relation is given by Hooke's law for linear elastic material is given by $\sigma_{ij} = Q_{ijkl}\varepsilon_{kl}$, where Q_{ijkl} is the material stiffness tensor.

Lastly, force equilibrium equations describe the static equilibrium of the body in the absence of body forces such as gravitation, expressed in strain, as $\partial\sigma_{ij}/\partial x_j = 0$.

11

Combining these three relations results in a system of equations that can be solved either analytically or numerically, depending on the complexity of the problem. A more detailed description of these three governing equations is given in appendix A.

2.3.2 Solution methods

Numerous analytical and numerical solution methods to the linear elastic governing equations have been derived and proposed, but except for relatively simple geometries and loads many of these rely on restrictive assumptions. Examples of common analytical methods include Euler-Bernoulli bending theory, Kirchoff-Love plate theory and Mindlin-Reissner plate theory. [25]

In heterogeneous materials such as composites made out of stacked laminae, the heterogeneous structure further complicates the solution process, and a variety of solution methods have been proposed to simplify and solve for these cases, among which Classical Lamination Theory (CLT) is a common choice if certain symmetries exist. A widely used method for complicated geometries or load cases is FEA due to the possibility to control parameters affecting the accuracy of the solution.

Finite Element Analysis

In preparing for running the finite element simulations the heterogeneous composite material first needs to be homogenized. Out of a large variety of homogenization schemes [9] proposes an explicit formulation of the effective material stiffness matrix based on the assumption that continuous strains and stresses through the thickness of the composite are equal to the strains and stresses in the homogenized cylinder, *i.e.*

$$\varepsilon_\varphi^i = \varepsilon_\varphi, \quad \varepsilon_z^i = \varepsilon_z, \quad \varepsilon_{\varphi z}^i = \varepsilon_{\varphi z}, \quad \sigma_r^i = \sigma_r, \quad \sigma_{rz}^i = \sigma_{rz}, \quad \sigma_{r\varphi}^i = \sigma_{r\varphi} \qquad (2.3)$$

for the ith ply, where lack of indices indicate the corresponding value for the homogenized cylinder. This assumption has been shown to be valid for thin to moderately thick-walled composites.

When a homogenized material stiffness matrix has been obtained, the geometry needs to be divided into a number of elements and nodes numbered according to a consistent scheme. In the case of tetrahedral elements, the `MATLAB` routine `delaunayTriangulation` can be used. As the routine name indicates it is based on the Delaunay algorithm for triangulation. [26].

Using the effective material stiffness matrix and the generated mesh, the governing equations can be discretized and an approximate solution for the displacement of the nodes during the excertion of certain loads can be obtained. For a conceptual outline of the Finite Element method used, see appendix B.

3

Method

A brief description of the methods used for conducting this project is given, as well as the materials used for measurements and experiments.

An extensive literature review about the current state of the art for composites and reinforced plastics initialized the project, as well as an investigation of the floorball market.

Using the gained knowledge of the field, the aim of the project was to successfully simulate the behavior of cylindrical composite laminates and its properties in order to maximize load-carrying capacity and impact resistance.

The overall procedure of the project can be described by three main categories:

- Identify structural properties of existing sticks by studying a collection of broken samples
- Research desirable material properties
  - Perform measurements on existing sticks
  - Perform movement analysis of sticks in use using `Qualisys Track Manager`
- Build and run a FEM implementation in `MATLAB` for geometries resembling those of floorball sticks

The end goal was reached by comparing material properties of different angle-ply composites, and researching the effects of the structure of the used composite matrix and reinforcements. Computer simulations, *e.g.* with FEM, was a largely preferred method for testing hypothetical composite structures, and the results thereof are a constituting part of the end result.

3.1 Experimental procedure

The aim of the experiment is to obtain the empirical relation between applied loads and the resulting deflections. Since the applied loads result in relatively small deflections linear elastic material response in the floorball sticks can be assumed.

In order to obtain a reference value to compare with the simulations, a three point bending test was used and the approximate deflection as a function of an applied load at the end of a stick with fixed support in the other end was obtained according to equation (2.1).

Furthermore, movement analysis data from recordings of slapshots provided by `Qualisys` was analyzed using `Qualisys Track Manager` and `MATLAB` in order to determine typical values of deflection.

3.2 Computational details

FEA was used to perform simulations of a hollow cylinder with fixed support in one end and applied load to the other. A `MATLAB` program was implemented based on FEM code developed in [27], modified to adhere to the currently investigated scenario. The FEM procedure was iterated over a number of different ply angles and stacking sequences.

The geometry of the problem can be seen in figure 2.2, while the dimensions of the cylindrical shell were taken as the typical dimensions of floorball sticks, as given in table 1.2, and material constants were set according to the values given in table 2.2.

3.2.1 Assumptions

A number of assumptions were made in order to simplify the problem statement, reducing its complexity and thereby making the problem solvable with reasonable effort.

First of all, the problem was stated as a static one, as opposed to the possible dynamic case. That is, the problem was viewed as time-independent, an instantaneous snapshot of a floorball slapshot at the moment when the load on the stick is at its maximum. While this leaves no possibility of studying the effect of vibrations in the stick, it eliminates the complexity presented from having time as a variable. Furthermore, it was assumed that the material studied is not subjected to hysteresis; it has no memory of previously applied stresses or strains. This is an indirect consequence of the assumption of time-independent behavior.

A common simplification in FEA is to assume linear behavior in the constitutive relations, *i.e.* linear elastic materials, something that was done in this case. In small geometric displacements carbon fiber reinforced plastics do indeed exhibit linear elastic properties. In the cases of large deflections non-linear elastic response and material failure occurs which complicates the matter substantially, but as a starting point the material was assumed to behave linearly elastic.

The effects of body forces were neglected due to their relatively small magnitudes compared to the applied loads under consideration.

3.2.2 Mesh generation

A mesh describing the geometry of a hollow cylindrical body was generated using Delaunay triangulation, resulting in a set of 4-noded tetrahedrons. The geometry took the values of a reference stick as listed in table 1.2, and unless otherwise stated the geometry was divided into 20 equally spaced nodes in the $\hat{z}$ and $\hat{\varphi}$ directions and 3 nodes in the radial ($\hat{r}$) direction.

3.2.3 Applied loads and boundary conditions

The applied load was assembled in the FEA to resemble that with which a floorball stick is subjected to during a slapshot. In order to simplify the application of the load, one end of the cylindrical shell was subjected to a boundary condition of zero displacement, representing the player's lower grip. The other end of the shell was subjected to a point load in the positive y-direction representing the force from the point of impact where the stick hits the floor. The remaining surfaces were subjected to Neumann conditions to simulate unconstrained displacement.

3.2.4 Problem formulation and solver implementation

The procedure of generating the complete stiffness matrix used in the Finite Element formulation is illustrated in figure 3.1.
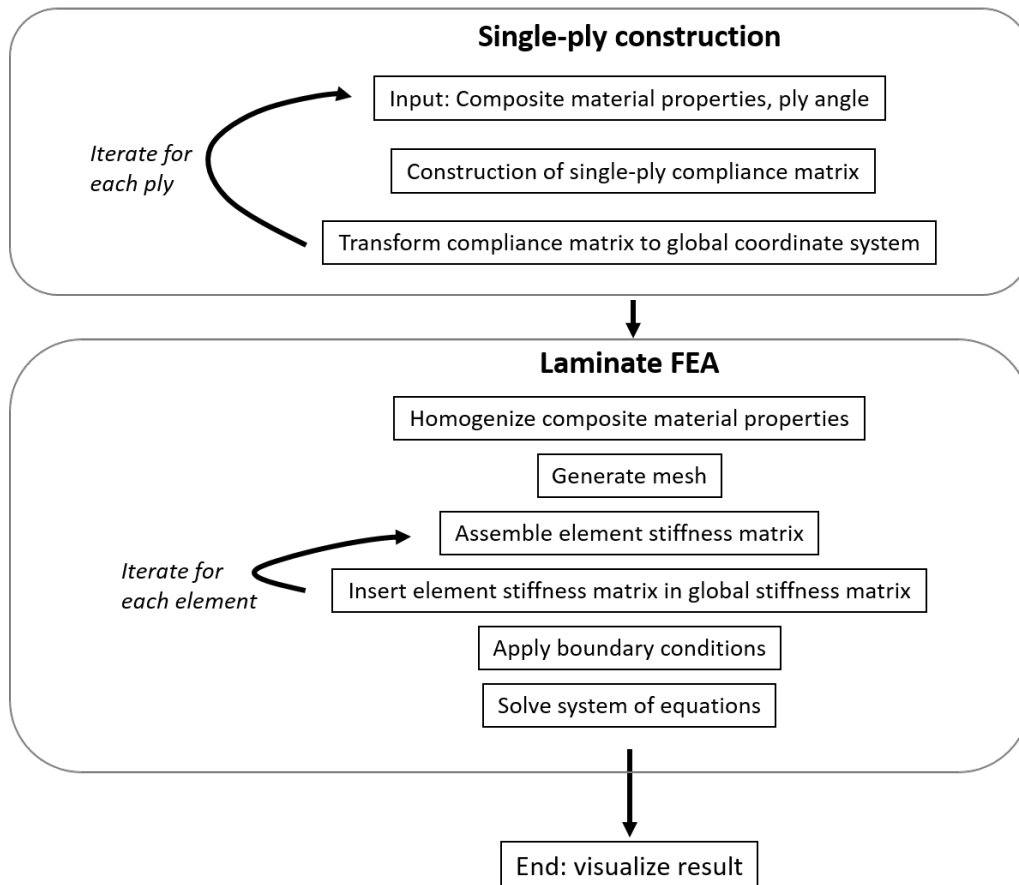

Figure 3.1: Implementation flowchart for Finite Element Method

In the case of a floorball stick, the fiber tows are aligned off-axis, and the stiffness matrix needs to be transformed into the global coordinate system accordingly [28]. Once the material stiffness matrix was transformed, the composite laminate was simulated as a continuous medium via a homogenization process, instead of considering it as a set of layers with different material properties. Following the procedure outlined in section A a

single ply stiffness matrix in the global coordinate system was obtained, with elements dependent on the ply angle θ. Thereafter the heterogeneous stack of plies was homogenized according to the scheme described in [9].

Following the generation of the mesh, applying of boundary conditions and assembly of the element and global stiffness matrices as outlined in B, the system of equations were solved resulting in a vector of displacements. The procedure was then iterated for different fiber orientations and laminate stacking sequences.

3.3   Processing results

The results from a three point bending test were used to calculate the theoretical deflection of a stick with fixed support in one end. These results were then compared to the deflection calculated from movement analysis measurements, and the combined values of applied forces and deflections were used for evaluating the FEA simulations.

4

Results

Typical stick deflections were calculated from movement analysis data and are depicted here along with results from experimental measurements. More importantly the outcome of the FEM simulations are outlined.

4.1 Deflection

A typical deflection of a floorball stick during a slapshot performed by a professional, male floorball player can be seen in figure 4.1 and amounts to approximately $190\,\mathrm{mm}$ upon impact. Several other movement analysis measurements are depicted in appendix C. As can be seen from these results, stick deflection from a professional male floorball player typically ranges from $190\,\mathrm{mm}$ to $220\,\mathrm{mm}$.

Three point deflection tests resulted in an approximate function for the deflection of a stick with fixed support in one end, depending on the applied load on the other end. This function is seen to be given by

$$w_{fix}\left(L_{fix}\right) = 16\frac{P_{fix}}{P_{3p}}\frac{L_{fix}^3}{L_{3p}^3}w_{3p}\left(L_{3p}/2\right) = K \cdot P_{fix}. \tag{4.1}$$

For the reference case, with L_{fix} set to $460\,\mathrm{mm}$, the value of K amounts to approximately $1.66 \cdot 10^{-4}$, while the estimated lower grip of $592\,\mathrm{mm}$ in figure 4.1 led to a value of $K = 3.53 \cdot 10^{-4}$. A plot of deflection versus applied force for the two cases can be seen in figure 4.2. As can be seen, the reference stick requires $1147\,\mathrm{N}$ to obtain a maximum deflection of $190\,\mathrm{mm}$, while the other case only requires a load of $538\,\mathrm{N}$ for the same deflection to occur.

4.2 Computational results

The used FEM program, developed in `MATLAB`, can be viewed and cloned from `https://github.com/MatsLindstrom/FEM_CFRP_hollowCylinders`.

The results from initial FEM simulations using nine zero angle plies ($[0]_9$) can be seen in
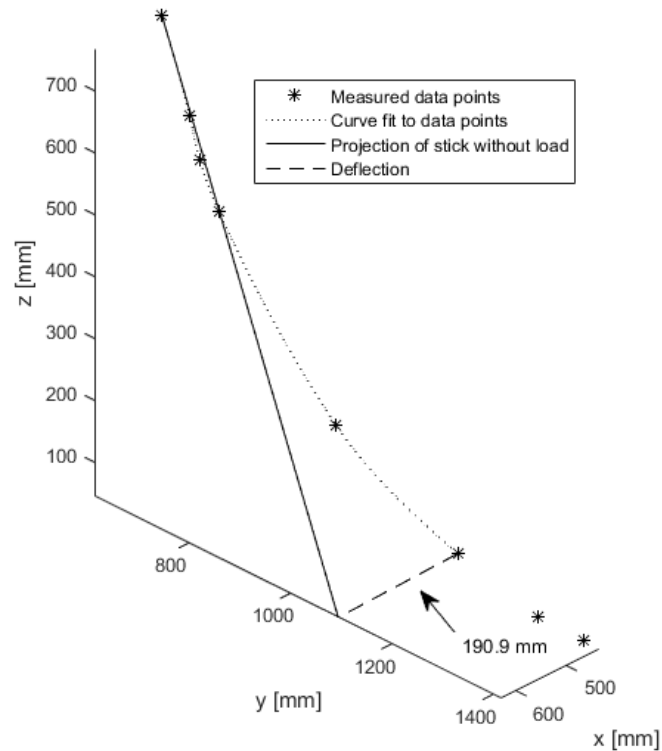
Figure 4.1: Typical deflection during slapshot performed by a professional, male floorball player

figure 4.3. As can be seen, the geometry deforms in the positive y-direction as intended. Following the calculations from simple bending of beams in section 4.1 the applied load in the reference case with cylinder length $460\,\text{mm}$ was set to $1147\,\text{N}$, resulting in a deflection of approximately $69.2\,\text{mm}$ as depicted in figure 4.3b.

Results from simple bending using the length $592\,\text{mm}$ as in the second considered case reveals that a load of $538\,\text{N}$ should be applied. This leads to the result shown in figure 4.3c and a maximum deflection of $57.3\,\text{mm}$.

Figure 4.4 shows a comparison of 10 different cases where the value of the largest ply angle θ relative to the cylinder's principal direction is varied according to the schemes outlined in table 4.1, using $\gamma = \theta/4$.

Case 1 through 4 (figure 4.4a) were chosen in order to enable comparison of a selection of the simplest possible setups, while case 5 and 6 (figure 4.4b) were chosen in order to further highlight the differences between symmetric and anti-symmetric ply stacking. Case 7 and 8 (figure 4.4c) were modeled for comparison between stacking sequences. Finally, case 9 and 10, depicted in figure 4.4d, were chosen in order to evaluate the effect of varying the number of plies and mesh refinement, respectively.
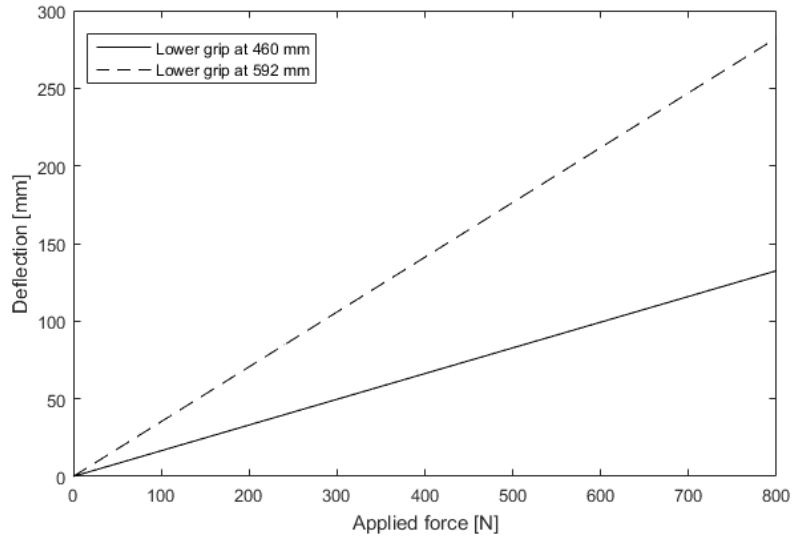
Figure 4.2: Theoretical deflections from simple bending relations

Table 4.1: Simulated cases for maximum angle θ, where $\gamma = \theta/4$

Case nr	Stacking sequence	Description
1	$[\theta]_9$	Constant angle θ
2	$[\pm\theta]_9$	Constant, alternating angle θ
3	$[\theta, \theta - \gamma, \theta - 2\gamma, \theta - 3\gamma, 0]_s$	Symmetric ply stacking
4	$[\theta, \theta - \gamma, \theta - 2\gamma, \theta - 3\gamma, 0]_a$	Anti-symmetric ply stacking
5	$[\theta - 3\gamma, \theta - 2\gamma, \theta - \gamma, \theta, 0]_s$	Symmetric, descending magnitude of ply angle
6	$[\theta - 3\gamma, \theta - 2\gamma, \theta - \gamma, \theta, 0]_a$	Anti-symmetric, descending ply angle
7	$[\pm(\theta - 2\gamma), \pm\theta, 0]_s$	Symmetric, ascending, alternating ply angle
8	$[\pm\theta, \pm(\theta - 2\gamma), 0]_s$	Symmetric, descending, alternating ply angle
9	$[\pm\theta]_{15}$	Increased number of plies
10	$[\pm\theta]_9$	Finer mesh (30 nodes in $\hat{z}$ and $\hat{\varphi}$ direction)

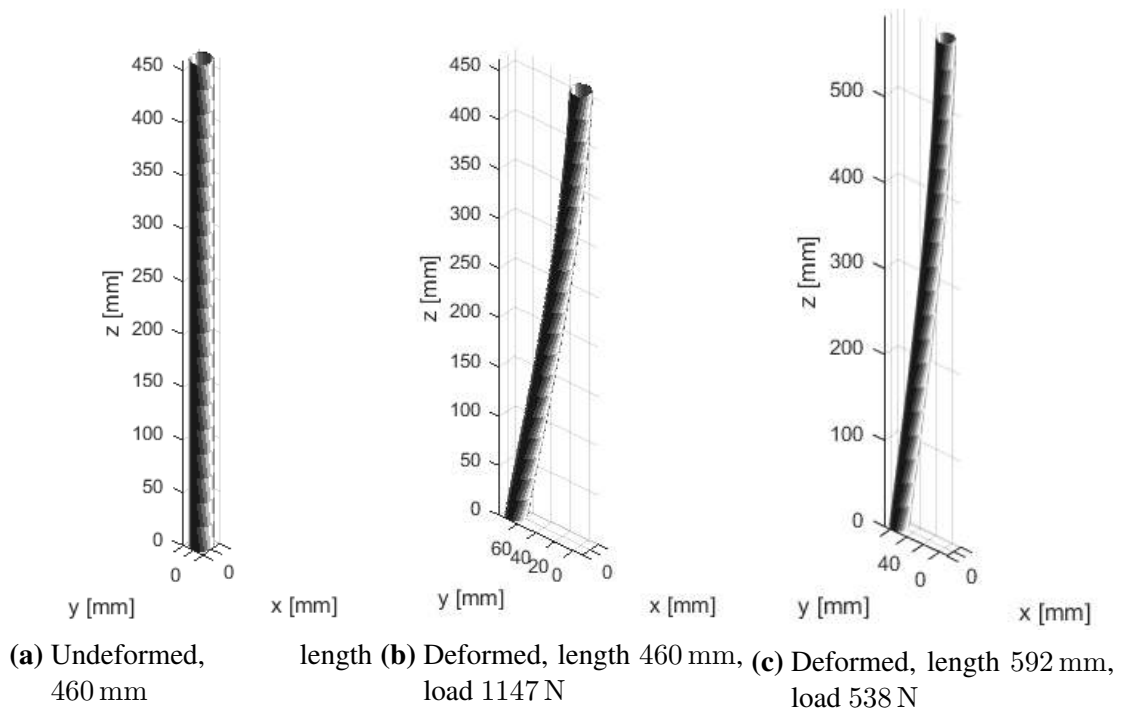**(a)** Undeformed, length 460 mm **(b)** Deformed, length 460 mm, load 1147 N **(c)** Deformed, length 592 mm, load 538 N
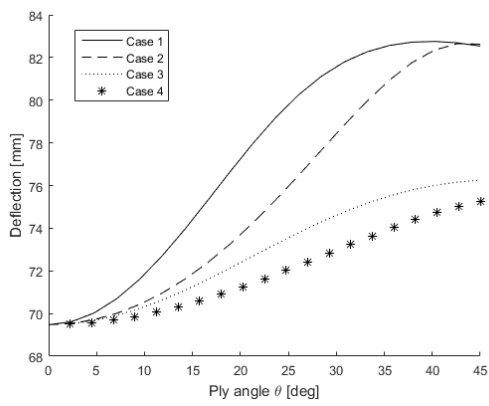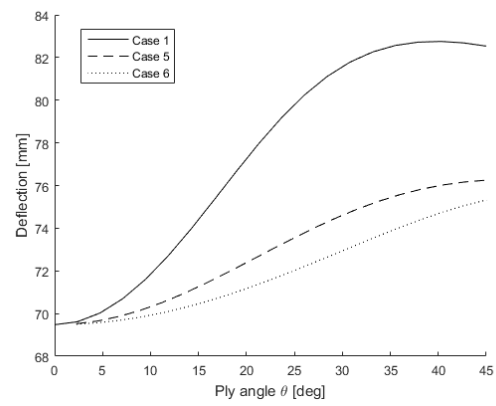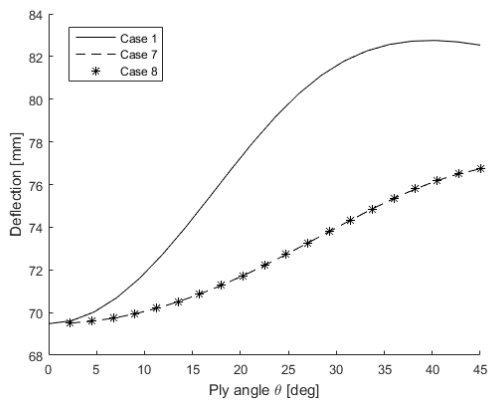
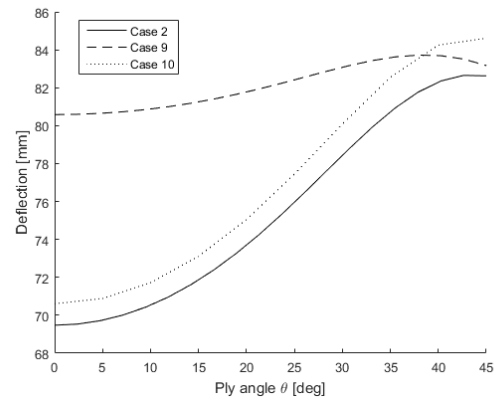**Figure 4.3:** FEM simulations, visualization

(a) Stacking of 9 plies

(b) Stacking of 9 plies

(c) Stacking of 9 plies

(d) Varying number of plies and mesh refinement

Figure 4.4: Results of simulations

5

Discussion

The following chapter presents possible errors and uncertainties introduced by the methods used. Furthermore, the results are analyzed and compared. Finally, suggestions for further research and possible paths for further development of this project is presented.

5.1   Experimental measurements

The deflections procured through the movement analysis data and simple bending theory are meant as reference values to compare with the simulation results, so in that sense the uncertainties introduced from the methods used are negligible under these circumstances.

5.2   Computational results

In order to increase accuracy and usefulness of computational results, certain aspects of the code should be developed. Also, the results produced in this report can still be interpreted relatively freely, due to the limited number of simulations performed. However, the more important aspect of the project purpose was to develop a code base that can provide a basis for further research, something that has been completed successfully.

5.2.1   Errors and uncertainties

The numerical approximation that is a natural part of FEA leads to a number of uncertainties. Some deviation could be caused by a phenomenon termed shear locking, resulting from the form of elements used and the placement of the nodes. Tetrahedrons might not be the best choice of elements for this FEM discretization. A suggestion is to instead generate a mesh of 8-noded or 20-noded hexahedron (brick) elements, even though the built-in Delaunay triangulation routine in `MATLAB` can not be used, making the numbering of nodes and elements a tedious procedure. Furthermore, the Gaussian integration might lead to too rough an approximation, choice of other shape functions (*e.g.* quadratic shape functions) and an increased number of integration points through changing element type could solve this issue, although this does increase the computational cost considerably.

Load uncertainties affect the result in practical use of these materials. Even if the value of $700\,\mathrm{N}$ has been established in previous work (see [16]), the real magnitude and direction of the applied load in game play can vary plenty.

Different homogenization schemes should be implemented to evaluate the performance of the specific scheme used in the current program. Furthermore, by using a sufficiently fine mesh the material need not be homogenized, although this greatly increases computational cost. If such a development is considered, care must be taken to have integration points inside the plies themselves and not only at the boundaries between plies.

Finally, a posteriori error estimation can be applied in order to evaluate how the solutions converge with respect to the true values.

5.2.2 Interpretation of results

Interpreting the computational results presented in section 4.2 leads to the following:

Figure 4.3 - simulation of the bending of a cylindrical hollow composite was successful. However, the results deviate greatly in magnitude from expected results. The expected deflection for the simulation shown in figure 4.3b was more than double of the obtained value. The same situation was seen to occur for the simulation in figure 4.3c. This deviation is most likely due to shear locking, but further simulations must be run in order to confirm this claim.

Running several further simulations leads to believe that the simulation results can be compared relative to each other. This conclusion is mainly supported by the shape of the curves presented in figures 4.4, where the direct link between increase in ply angle and increase in maximum deflection follows from intuitive reasoning.

Figure 4.4a - as expected, varying the angles in a $\pm$ configuration leads to smaller deflections. Intuitively, this should be a result of the elimination of a preferential material direction. This conclusion is further supported by the result that the anti-symmetric material in case 4 also shows smaller deflection than its symmetric equivalent in case 3.

Figure 4.4b - also here the previously stated conclusion, that anti-symmetric ply stacking leads to less deflection, is confirmed.

Figure 4.4c - varying the order of the stacking sequence while keeping the angle configuration set results in nearly identical curves, leading to the belief that the stacking sequence does not greatly affect the deflection.

Figure 4.4d - these results show how increasing the number of plies seems to lead to higher deflection. Since the total thickness of the material remained constant, increasing the number of plies led to decreasing the thickness of each ply, and thus it stands to reason that thinner individual plies lead to greater deflections. While refining the mesh for the simulation did alter the magnitude of the deflection slightly, it can be seen that the shape of the curve remains intact, and thus it can be concluded that mesh refinement did not affect the results much, although it did greatly increase the computational cost, increasing the time for a simulation to run approximately by a factor of 5.

To summarize, FEM can efficiently be used to simulate the effects of varying material

properties and structure for hollow cylinders. The largest implications these results have on the development of fiber reinforced materials for use in floorball stick shafts can be listed as follows:

- Ply stacking sequence has a relatively small effect in the dimensions considered
- Ply angle configuration plays an important part in the optimization process, and a large part of the fibers should be aligned parallel or close to parallel to the direction of the greatest applied strain
- The number and/or thickness of the individual plies are of considerable importance since thinner plies leads to larger deflections

5.3 Further research

The material presented in this report has but scratched the surface of the research possibilities related to floorball stick shaft performance. In future work, the code here developed can be reused to investigate several important aspects of material performance relevant for floorball stick shafts, but also completely different paths can be taken in order to gain further knowledge in the field. Besides work that can be done on improving the overall performance of the current code base as stated in section 5.2.1, the following subsections outline other research possibilities.

5.3.1 Developing the current project

By applying failure criterion such as a maximum strain or maximum stress criteria failure load analysis can be performed, either for the homogenized material as a whole or for each individual ply until complete material failure occurs.

Many common composite materials on the market today consist of interwoven fibers, as opposed to the helically orthogonal configurations studied in this project. By studying the microstructure of these weaves it is possible to approximate its macroscopic behavior.

Producing different shaft geometries is an increasingly popular method for increasing the stick performance in floorball today, and such geometries can relatively easily be implemented in the current setup.

From the current implementation it is straightforward to calculate approximate stresses and strains in the cylinders, and a next step in the project could be the developing of a subroutine that automatically performs these calculations.

5.3.2 Alternative research paths

Among the great number of aspects that can be considered in future work, some of the more interesting (author's opinion) include investigating delamination between plies [29], the potential use of carbon nanofibers [30], or fatigue resistance in real sticks. The latter might be done by subjecting sticks to cyclic loads over a longer period of time. Another

method that can be used to research the strain response of floorball sticks, which could be done through strain gauge measurements. In this case it is recommended to use a Wheatstone half-bridge, thus measuring tension and compression simultaneously, in order to increase accuracy.

6

Conclusion

Finally, it can be stated that the simulation of floorball stick shafts with respect to lamina stacking configurations is possible using the Finite Element Method, although initial simulations suggest that accuracy must be increased in order to produce more reliable results.

Initial simulations can confirm the intuitive result that orienting the fiber along the axis of bending reduces the deflection. Furthermore, it has been concluded that antisymmetric ply stackings should lead to smaller deflection of the shaft compared to equivalent symmetric stacking angles. It can also be seen that refining the mesh above a certain number of nodes does not significantly affect the accuracy of the result, while increasing the number of plies in the material greatly affects the deflection.

Bibliography

[1] Wilde J, Lundin U. Chalmers blir riksidrottsuniversitet [homepage on the Internet]. Gothenburg, Sweden: Chalmers University of Technology; 2015 [updated 2015 Jun 15; cited 2015 Sep 05]. Available from: `http://www.chalmers.se/sv/nyheter/Sidor/Chalmers-far-riksidrottsuniversitet.aspx`.

[2] Chalmers Sport & Teknologi, Innebandy [homepage on the Internet]. Gothenburg, Sweden: Chalmers Area of Advance, Materials Science; 2015 - [cited 2015 Oct 10]. Available from: `http://www.sportteknologi.se/innebandy`.

[3] IFF Today and History in Short [homepage on the Internet]. Helsinki, Finland: International Floorball Federation; 2015 [cited 2015 Sep 05]. Available from: `http://www.floorball.org/pages/EN/IFF-Today-and-History-in-short`.

[4] SP Technical Research Institute of Sweden. Material regulations, certification rules for IFF-marking of floorball equipment. Helsinki, Finland; 2013. SPCR 011.

[5] Easterling KE. Advanced Materials for Sports Equipment. 1st ed. Dordrecht: Springer-Science+Business Media, B.V.; 1993.

[6] Abdi B, Mozafari H, Ayob A, Kohandel R. Buckling Behavior of Clamped Laminated Composite Cylindrical Shells under External Pressure Using Finite Element Method. Applied Mechanics and Materials. 2012;121-126:43–47.

[7] Adali S. Design Optimization of Composite Laminates under Deterministic and Uncertain Conditions. In: Advani SG, Shonaike GO, editors. Advanced Polymeric Materials, Structure Property Relationships. Boca Raton, FL: CRC Press LLC; 2003. .

[8] Music E, Widroth A. Modelling of Spread Tow Carbon Fabric Composites for Advanced Lightweight Products. Chalmers University of Technology; 2013.

[9] Sun XS, Tan VBC, Chen Y, Tan LB, Jaiman RK, Tay TE. Stress analysis of multi-layered hollow anisotropic composite cylindrical structures using the homogenization method. Acta Mechanica. 2014;225(6):1649–1672.

[10] International Floorball Federation, Rules and Competition Committee. Rules of the game, Rules and Interpretation. Helsinki, Finland; 2013.

[11] Development & Innovations [homepage on the Internet]. Mölnlycke, Sweden: RE-NEW GROUP SWEDEN AB; c2011 [cited 2015 Sep 06]. Available from: `http://www.zone.se/DEVELOPMENT-&-INNOVATIONS.html#start`.

[12] Shaft Techniques [homepage on the Internet]. Mölnlycke, Sweden: RENEW GROUP SWEDEN AB; c2011 [cited 2015 Sep 06]. Available from: `http://www.unihoc.se/shaft_technology.html?`

[13] Salming Performance Technologies [homepage on the Internet]. Askim, Sweden: Salming Sports; c2015 [cited 2015 Sep 06]. Available from: `http://www.salming.com/en/floorball/technologies/`.

[14] Sticks [homepage on the Internet]. Espoo, Finland: Exel; c2013 [cited 2015 Sep 06]. Available from: `http://www.exelsports.com/app/product/list/-/id/9`.

[15] Tekniska specifikationer [homepage on the Internet]. Piteå, Sweden: Oxdog; c2015 [cited 2015 Sep 06]. Available from: `http://www.oxdog.net/sv/technologies/`.

[16] Karlsson J. Analysis of floorball sticks using high speed camera and Abaqus. Chalmers University of Technology; 2011.

[17] McCrum NG, Bucknall CB, Buckley CP. Principles of polymer engineering. 2nd ed. Oxford: Oxford University Press; 1997.

[18] Andrews R, Jacques D, Rao AM, Rantell T, Derbyshire F, Chen Y, et al. Nanotube composite carbon fibers. Applied Physics Letters. 1999;75(9):1329–1331.

[19] Bhattacharyya AR, Sreekumar TV, Liu T, Kumar S, Ericson LM, Hauge RH, et al. Crystallization and orientation studies in polypropylene/single wall carbon nanotube composite. Polymer. 2003;44:2373–2377.

[20] Bacon R, Silvaggi AF. Electron microscope study of the microstructure of carbon and graphite fibers from a rayon precursor. Carbon. 1971;9:321–325.

[21] Hugo JA, Phillips VA, Roberts BW. Intimate Structure of High Modulus Carbon Fibres. Nature. 1970;226:144.

[22] Chand S. Review; Carbon fibers for composites. Journal of Materials Science. 2000;35(6):1303–1313.

[23] Hawthorne HM, Baker C, Bentall RH, Linger KR. High Strength, High Modulus Graphite Fibres from Pitch. Nature. 1970;227(5261):946–947.

[24] Nordling C, Österman J. Physics handbook for science and engineering. Lund: Studentlitteratur; 2006.

[25] Rand O, Rovenski V. Analytical methods in anisotropic elasticity: with symbolic computational tools. Boston: Birkhäuser; 2005.

[26] delaunayTriangulation class [homepage on the Internet]. The MathWorks, Inc.; c1994-2015 [cited 2015 Oct 11]. Available from: `http://se.mathworks.com/help/matlab/ref/delaunaytriangulation-class.html?refresh=true`.

[27] Alberty J, Carstensen C, Funken SA, Klose R. Matlab implementation of the finite element method in elasticity. Computing. 2002;69(3):239–263.

[28] Romashchenko VA. Solutions of dynamic problems for incompressible and slightly compressible helically orthotropic non-uniform thick-walled cylinders. Journal of Applied Mathematics and Mechanics. 2007;71(1):52–60.

[29] Khokhar ZR, Ashcroft IA, Silberschmidt VV. Simulations of delamination in CFRP laminates: Effect of microstructural randomness. Computational Materials Science. 2009;46(3):607–613.

[30] Kumar S, Doshi H, Srinivasarao M, Park JO, Schiraldi DA. Fibers from polypropylene/nano carbon fiber composites. Polymer. 2002;43(5):1701–1703.

[31] Romashchenko VA, Beiner OS, Babich YN. Numerical-Analytical Method For 3D Dynamics Study of Spirally Orthotropic Multilayer Cylinders. Strength of Materials. 2011;43(4):438–446.

[32] Johnson C. Numerical solution of partial differential equations by the finite element method. Mineola, NY: Dover Publications Inc.; 2009.

Appendices

A

Governing equations for helically orthogonal plies

The force equilibrium equations for the static case neglecting body forces in cylindrical coordinates are given in [31] as

$$\frac{\partial \sigma_x}{\partial x} + \frac{\partial \sigma_{xy}}{\partial y} + \frac{\partial \sigma_{zx}}{\partial z} = 0$$
$$\frac{\partial \sigma_{xy}}{\partial x} + \frac{\partial \sigma_y}{\partial y} + \frac{\partial \sigma_{yz}}{\partial z} = 0 \qquad\qquad \text{(A.1)}$$
$$\frac{\partial \sigma_{zx}}{\partial x} + \frac{\partial \sigma_{yz}}{\partial y} + \frac{\partial \sigma_z}{\partial z} = 0$$

In Voigt notation, the strain-displacement relation is given by

$$\boldsymbol{\varepsilon} = \begin{pmatrix} \varepsilon_x \\ \varepsilon_y \\ \varepsilon_z \\ 2\varepsilon_{xy} \\ 2\varepsilon_{yz} \\ 2\varepsilon_{zx} \end{pmatrix} = \begin{pmatrix} \frac{\partial}{\partial x} & 0 & 0 \\ 0 & \frac{\partial}{\partial y} & 0 \\ 0 & 0 & \frac{\partial}{\partial z} \\ \frac{\partial}{\partial y} & \frac{\partial}{\partial x} & 0 \\ 0 & \frac{\partial}{\partial z} & \frac{\partial}{\partial y} \\ \frac{\partial}{\partial z} & 0 & \frac{\partial}{\partial x} \end{pmatrix} \begin{pmatrix} u \\ v \\ w \end{pmatrix} = \boldsymbol{R}\boldsymbol{u} \qquad\qquad \text{(A.2)}$$

For a general anisotropic linear elastic material the stress-strain relationship is given by

$$\sigma_{ij} = Q_{ijkl} \left(\varepsilon_{kl} - \alpha_{kl} \Delta T \right) \qquad\qquad \text{(A.3)}$$

where Q is the fourth-order elastic stiffness tensor and α is the thermal expansion coefficient tensor. The stiffness tensor has, in its most general form, 81 components. However, due to symmetry $Q_{ijkl} = Q_{klij} = Q_{jikl} = Q_{ijlk}$, which reduces the number of independent components to 21.

Under the assumption of constant temperature, the general stress-strain relation in matrix form (Voigt notation) for an anisotropic linear elastic material in cylindrical coordinates $(\hat{r}, \hat{\varphi}, \hat{z})$ reduces to

$$\boldsymbol{\sigma} = \begin{pmatrix} \sigma_r \\ \sigma_\varphi \\ \sigma_z \\ \sigma_{\varphi z} \\ \sigma_{rz} \\ \sigma_{r\varphi} \end{pmatrix} = \begin{pmatrix} Q_{11} & Q_{12} & \cdots & Q_{16} \\ Q_{12} & Q_{22} & \cdots & Q_{26} \\ \vdots & \vdots & \ddots & \vdots \\ Q_{16} & Q_{26} & \cdots & Q_{66} \end{pmatrix} \begin{pmatrix} \varepsilon_r \\ \varepsilon_\varphi \\ \varepsilon_z \\ 2\varepsilon_{\varphi z} \\ 2\varepsilon_{rz} \\ 2\varepsilon_{r\varphi} \end{pmatrix} = \boldsymbol{Q}\boldsymbol{\varepsilon} \tag{A.4}$$

where $\boldsymbol{Q}$ represents the stiffness matrix. Similarly, the inverse relationship can be written as $\varepsilon = \boldsymbol{C}\boldsymbol{\sigma}$ with $\boldsymbol{C}$ being the compliance matrix.

In the case of a cylindrical ply with ply angle deviating from the principal direction of the cylinder, the stiffness matrix first has to be written in the plies local coordinate system, in which case it can be written in the same form as that of a cylindrical orthotropic material's:

$$\boldsymbol{Q} = \begin{pmatrix} Q_{rr} & Q_{r\varphi} & Q_{rz} & 0 & 0 & 0 \\ Q_{\varphi r} & Q_{\varphi\varphi} & Q_{\varphi z} & 0 & 0 & 0 \\ Q_{zr} & Q_{z\varphi} & Q_{zz} & 0 & 0 & 0 \\ 0 & 0 & 0 & 2G_{\varphi z} & 0 & 0 \\ 0 & 0 & 0 & 0 & 2G_{rz} & 0 \\ 0 & 0 & 0 & 0 & 0 & 2G_{r\varphi} \end{pmatrix} \tag{A.5}$$

The equivalent compliance matrix for a cylindrical anisotropic material is given by

$$\boldsymbol{C} = \begin{pmatrix} \frac{1}{E_{rr}} & -\frac{\nu_{\varphi r}}{E_{\varphi\varphi}} & -\frac{\nu_{zr}}{E_{zz}} & 0 & 0 & 0 \\ -\frac{\nu_{r\varphi}}{E_{rr}} & \frac{1}{E_{\varphi\varphi}} & -\frac{\nu_{z\varphi}}{E_{zz}} & 0 & 0 & 0 \\ -\frac{\nu_{rz}}{E_{rr}} & -\frac{\nu_{\varphi z}}{E_{\varphi\varphi}} & \frac{1}{E_{zz}} & 0 & 0 & 0 \\ 0 & 0 & 0 & \frac{1}{G_{\varphi z}} & 0 & 0 \\ 0 & 0 & 0 & 0 & \frac{1}{G_{rz}} & 0 \\ 0 & 0 & 0 & 0 & 0 & \frac{1}{G_{r\varphi}} \end{pmatrix} \tag{A.6}$$

where E_{ii} and ν_{ij} is the elastic modulus and Poisson's ratio in the ply's principal axes, $i,j = \{r,\varphi,z\}$.

The transformation to global cylindrical coordinates follows from the reasoning in [9], so that the transformed compliance matrix for the ith helical laminae with off-axis angle θ can be written as

$$\bar{\boldsymbol{C}}^{(i)} = \left(\boldsymbol{T}_\theta^{(i)}\right)^T \boldsymbol{C}^{(i)} \boldsymbol{T}_\theta^{(i)} \tag{A.7}$$

where the transformation matrix $\boldsymbol{T}_\theta^{(i)}$ is given by

$$
\boldsymbol{T}_\theta^{(i)} = \begin{pmatrix}
1 & 0 & 0 & 0 & 0 & 0 \\
0 & \cos^2 \theta^{(i)} & \sin^2 \theta^{(i)} & -\sin 2\theta^{(i)} & 0 & 0 \\
0 & \sin^2 \theta^{(i)} & \cos^2 \theta^{(i)} & \sin 2\theta^{(i)} & 0 & 0 \\
0 & \frac{1}{2}\sin 2\theta^{(i)} & -\frac{1}{2}\sin 2\theta^{(i)} & \cos 2\theta^{(i)} & 0 & 0 \\
0 & 0 & 0 & 0 & \cos \theta^{(i)} & \sin \theta^{(i)} \\
0 & 0 & 0 & 0 & -\sin \theta^{(i)} & \cos \theta^{(i)}
\end{pmatrix}
\tag{A.8}
$$

B

Finite Element discretization

Define a domain Ω with boundary Γ. On this domain, determine the displacement $\boldsymbol{u} = (u, v, w)$ and the symmetric stress tensor σ_{ij} under external loads f acting on the boundary. σ_{ii} represents normal stresses, while σ_{ij}, $i \neq j$, implies shear stresses. The values of $\boldsymbol{u}$ are interpolated using linear shape functions N_a, *i.e.*

$$\boldsymbol{u}_j = \sum_{a=1}^{n} N_a u_j^a = \boldsymbol{N}\boldsymbol{U} \tag{B.1}$$

for the ath node, where n is the number of nodes in the element and j is the considered dimension $j \in \{x, y, z\}$. The shape functions are written in terms of normalized local coordinates (ξ_1, ξ_2, ξ_3) as

$$N_1 = \xi_1, \quad N_2 = \xi_2, \quad N_3 = \xi_3, \quad N_4 = 1 - \xi_1 - \xi_2 - \xi_3. \tag{B.2}$$

From the strain-displacement relation in equation (A.2), this results in the system of equations

$$\boldsymbol{\varepsilon} = \boldsymbol{R}\boldsymbol{u} = \boldsymbol{R}\boldsymbol{N}\boldsymbol{U} = \boldsymbol{B}\boldsymbol{U}. \tag{B.3}$$

The elements in $\boldsymbol{B}$ contain derivatives of the shape functions,

$$\frac{\partial N_a}{\partial x_j} = \frac{\partial N_a}{\partial \xi_i} \frac{\partial \xi_i}{\partial x_j}, \tag{B.4}$$

where the first factor is easily deduced from equation (B.2), and the second factor follows from

$$x_i = \sum_{a=1}^{n} N_a x_i^a \quad \Rightarrow \quad \frac{\partial x_i}{\partial \xi_j} = \sum_{a=1}^{n} \frac{\partial N_a}{\partial \xi_j} x_i^a \quad \Rightarrow \quad \frac{\partial \xi_j}{\partial x_i} = \left[\sum_{a=1}^{n} \frac{\partial N_a}{\partial \xi_j} x_i^a\right]^{-1} \tag{B.5}$$

The principle of virtual work leads to the total strain energy written, using the constitutive relation $\sigma_{ij} = Q_{ijkl}\varepsilon_{kl}$, as

$$\delta\boldsymbol{W} = \int_{\Omega} \delta\boldsymbol{\varepsilon}^{T}\boldsymbol{\sigma}\,\mathrm{d}V = \int_{\Omega} [\boldsymbol{B}_{i}\delta\boldsymbol{U}_{i}]^{T}\,\boldsymbol{Q}\boldsymbol{B}_{j}\boldsymbol{U}_{j}\mathrm{d}V = \delta\boldsymbol{U}_{i}^{T}\int_{\Omega}\boldsymbol{B}_{i}^{T}\boldsymbol{Q}\boldsymbol{B}_{j}\mathrm{d}V\boldsymbol{U}_{j}. \qquad \text{(B.6)}$$

The increase in energy $\delta\boldsymbol{W}$ must equal the work done by external forces, and so

$$\delta\boldsymbol{W} = \delta\boldsymbol{U}_{i}^{T}\boldsymbol{f}_{i}. \qquad \text{(B.7)}$$

Equating (B.6) and (B.7), we get

$$\left[\int_{\Omega}\boldsymbol{B}_{i}^{T}\boldsymbol{Q}\boldsymbol{B}_{j}\mathrm{d}V \right]\boldsymbol{U}_{j} = \boldsymbol{f}_{i} \qquad \text{(B.8)}$$

where the term inside the brackets is called the element stiffness matrix A_{m} for the mth element. This integral can be approximated by evaluating it at select points within each element, here chosen to be at the barycenter of each element face and, in the case of surface elements, at the surface edge centers. Ultimately, the element stiffness matrix can now be written as

$$\boldsymbol{A}_{m} = \sum_{i=1}^{n} w_{i}\,|J|\,\boldsymbol{B}_{i}^{T}\boldsymbol{Q}\boldsymbol{B}_{j} \qquad \text{(B.9)}$$

where $|J|$ denotes the determinant of the Jacobian and w is the weight factor dependent on the number of integration points in the element, in the case of 4-noded tetrahedrons $w = 1/6$. Assembling the element stiffness matrices into one global stiffness matrix one obtains the system of equations

$$\boldsymbol{A}\boldsymbol{U} = \boldsymbol{f} \qquad \text{(B.10)}$$

where $\boldsymbol{A}$ is the global stiffness matrix, $\boldsymbol{U}$ is the vector of displacements to be solved for and $\boldsymbol{f}$ is a vector describing the boundary conditions. [32]

C

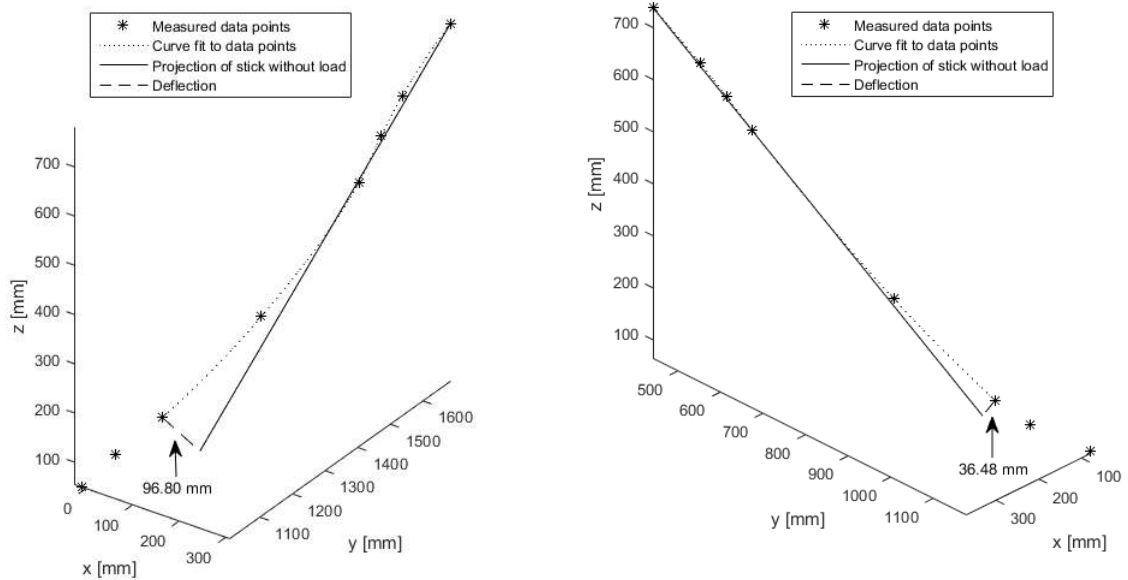# Stick deflections from movement analysis data

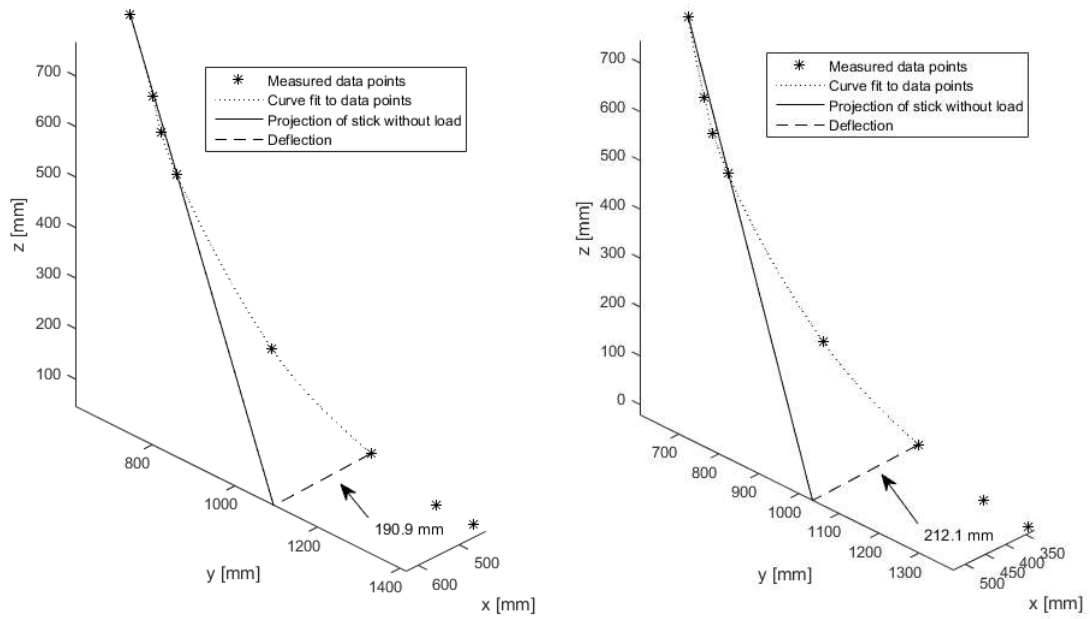**Figure C.1:** Deflections from movement analysis data

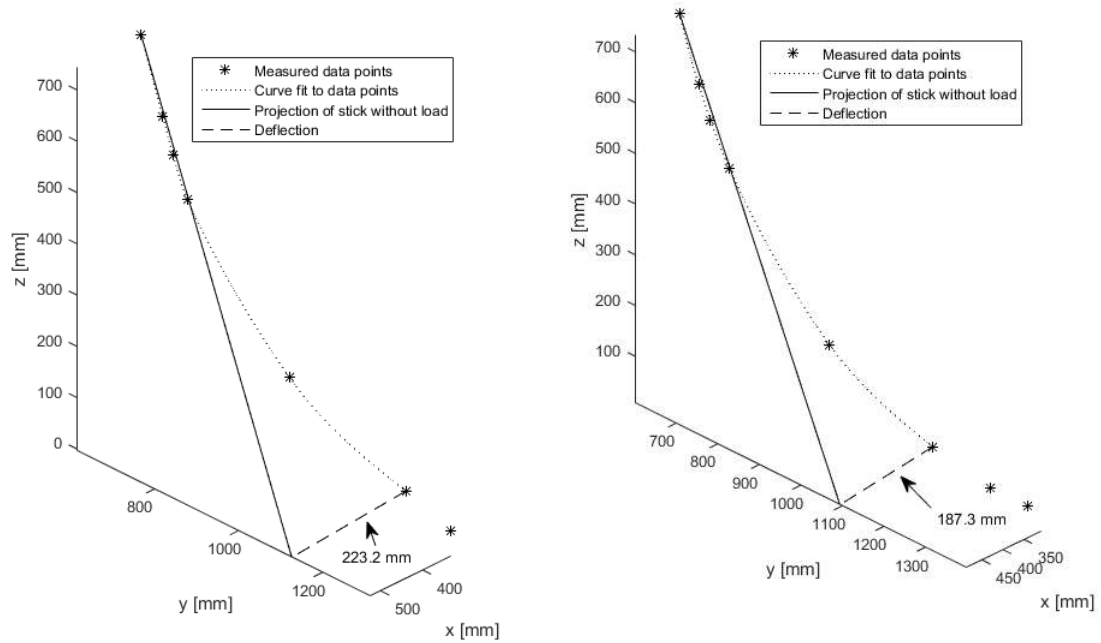**Figure C.2:** Deflections from movement analysis data

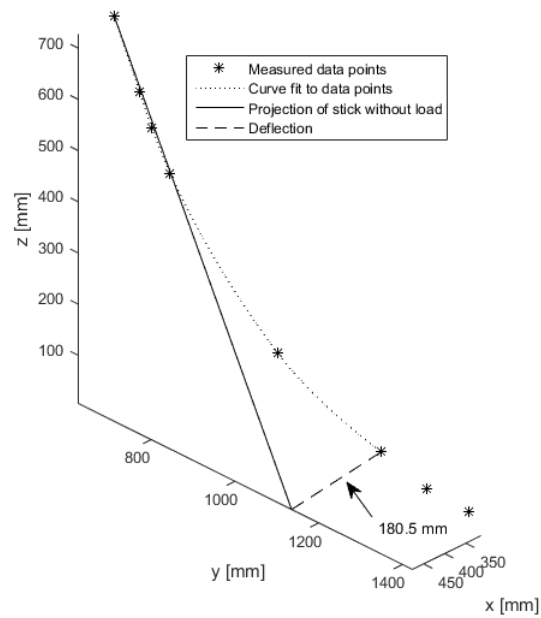
Figure C.3: Deflections from movement analysis data

Figure C.4: Deflection from movement analysis data